Analysis of drought and flood basins over the Limpopo River Basin in southern Africa

WATERWORKS EU – IMDROFLOOD Project

Report

to the Water Research Commission

by

CJC Reason

Department of Oceanography, University of Cape Town

Report no. 2618/1/20
ISBN 978-0-6392-0210-5

November 2020

Obtainable from:

Water Research Commission

Private Bag X03

Gezina, 0031

South Africa

orders@wrc.org.za or download from www.wrc.org.za

The Imdroflood project, led by Prof S Vicente of Consejo Superior de Investigaciones Científicas, Zaragoza, Spain, comprised a number of European collaborators and the Department of Oceanography at the University of Cape Town (UCT). It involved the analysis of flood and drought basins over several European catchment basins, as well as the Limpopo River Basin in southern Africa. Funding was provided by the European Union’s Joint Programming Initiatives (JPI) Waterworks programme, with the funds due to UCT channelled through the Water Research Commission (WRC).

DISCLAIMER

This report has been reviewed by the Water Research Commission (WRC) and approved for publication. Approval does not signify that the contents necessarily reflect the views and policies of the WRC, nor does mention of trade names or commercial products constitute endorsement or recommendation for use.

EXECUTIVE SUMMARY

An analysis of heavy rainfall events over the Limpopo River Basin during the summer has shown that these events are more common between January and March than between October and December. A sharp rainfall gradient exists across the region, which is related to the topography and distance from moisture sources. Tropical extratropical cloud bands make the largest contribution overall and are most common in February. The second-largest contribution comes from tropical low-pressure systems that peak in February. Mesoscale convective systems can make a substantial contribution in any summer month, whereas cut-off lows are more likely in October and March.

In terms of the interannual and interdecadal variability of the rainfall in the basin, an important aspect is the Botswana high-pressure system (Botswana High). This high-pressure system is a mid-level anticyclone that forms in the austral spring over western tropical southern Africa and then moves south and strengthens during summer. The relationships between low-frequency variability in this circulation system, regional rainfall, air temperature and sea surface temperature were examined. Multidecadal epochs in rainfall over southern Africa appear related to the strength and position of the Botswana High. This low-frequency variability may sometimes oppose and – at other times – reinforce trends in regional rainfall and temperature associated with global warming.

Although no students were formally funded by the project, a black South African student has been involved in the rainfall analysis over the Limpopo River Basin.

ACKNOWLEDGEMENTS

Funding from the European Union's Joint Programming Initiatives (JPI) Waterworks programme, administered by the Water Research Commission (WRC), is gratefully acknowledged. The comments of anonymous reviewers on the journal articles published from this project are also gratefully acknowledged.

Data was obtained from National Center for Environmental Prediction (NCEP)/National Center for Atmospheric Research (NCAR) reanalysis, the Climate Hazards Infrared Precipitation with Stations project and the Global Precipitation Climatology Project.

CONTENTS

LIST OF FIGURES

LIST OF TABLES

LIST OF ABBREVIATIONS AND ACRONYMS

CB	Cloud band
CHIRPS	Climate Hazards Infrared Precipitation with Stations
COL	Cut-off low
ENSO	El Niño Southern Oscillation
GHRSST	Group for High Resolution Sea Surface Temperature
GPCP	Global Precipitation Climatology Project
GridSat	Gridded Satellite
IBTrACS	International Best Track Archive for Climate Stewardship
ITCZ	Intertropical Convergence Zone
JPI	Joint Programming Initiatives
MC/MCS	Mesoscale Convective System
NCAR	National Center for Atmospheric Research
NCEP	National Centers for Environmental Prediction
NOAA	National Oceanic and Atmospheric Administration
OLR	Outgoing longwave radiation
SAM	Southern Annular Mode
SAWS	South African Weather Service
SIOD	South Indian Ocean Dipole
SLP	Sea level pressure
SST	Sea surface temperature
TL	Tropical low
TRM	Time residual mean
TRMM	Tropical Rainfall Measuring Mission
TTT	Tropical temperate trough
UCT	University of Cape Town
WRC	Water Research Commission

CHAPTER 1: EXTREME RAINFALL EVENTS OVER THE LIMPOPO RIVER BASIN

Located centrally within subtropical southern Africa, defined here as Africa south of 15 °S, is the Limpopo River Basin (Figure 1.1), an important region locally due to its agricultural output, rich biodiversity and tourism. The Limpopo River Basin mostly comprises a rural population, and extends about 1,770 km across four countries (southeastern Botswana, southern Zimbabwe, northeastern South Africa and southern Mozambique) where the Limpopo River flows into the southwestern Indian Ocean near the town of Xai-Xai. The altitude of the Limpopo River Basin ranges from less than 200 m over the Mozambican floodplains to higher than 1,600 m over the mountainous regions of South Africa. The rainfall season occurs between October and April, with the largest precipitation occurring during the late summer months (January to March) and the greatest evaporation losses occurring during the early summer (October to December). Both severe drought and extreme rainfall events are common over the Limpopo River Basin (Mulenga et al., 2003; Usman and Reason, 2004; Reason and Jagadheesha, 2005; Malherbe et al., 2014; Manhique et al., 2015).

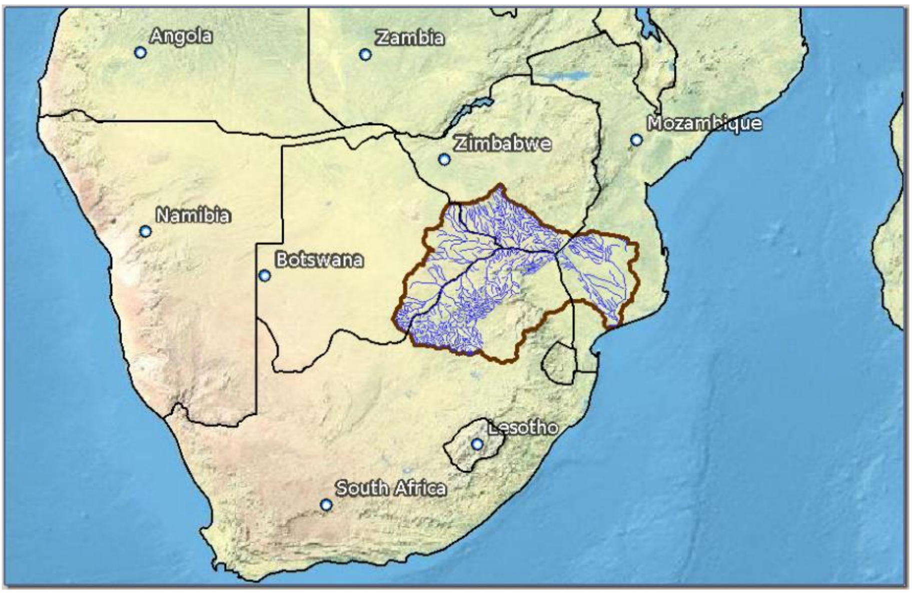

Figure 1.1: Topographic shaded relief map of southern Africa showing the Limpopo River Basin (brown polygon with rivers and tributaries) over parts of eastern Botswana, southern Zimbabwe, southwestern Mozambique, and northeastern South Africa. Produced with the National Oceanic and Atmospheric Administration's Weather and Climate Toolkit (after Rapolaki et al., 2019)

During the austral summer, southern Africa may experience extreme precipitation events associated with convective storms, ranging in scale from single-cell storms through to organised systems such as mesoscale convective complexes (Blamey and Reason, 2012; Blamey and Reason, 2013), squall lines (Rouault et al., 2002) and tropical storms (Reason and Keibel, 2004; Reason, 2007; Malherbe et al., 2012; Malherbe et al., 2014; Rapolaki and Reason, 2018). The dominant rainfall-producing systems over the region are synoptic-scale cloud bands, known locally as tropical temperate troughs (TTTs) (Harrison, 1984; Reason et al., 2006; Hart et al., 2010; Hart et al., 2013; Manhique et al., 2011). Cut-off lows (COLs) can also lead to extreme rainfall in the region (Taljaard, 1985; Singleton and Reason, 2006; Singleton and Reason, 2007a; Favre et al., 2012).

Many of these heavy rainfall events are associated with major socio-economic impacts, including sometimes loss of life. For example, the tropical cyclone Eline caused severe flooding over the basin when it tracked across Zimbabwe in February 2000 after making landfall near Beira on the central Mozambican coast (Dyson and Van Heerden, 2001; Reason and Keibel, 2004). About 1,000 people were killed as a result of this cyclone. Another notable flood event occurred in January 2013, which Manhique et al. (2015) suggested was related to an intense and long-lasting cloud band. The flood left approximately 200,000 people homeless and led to more than 100 deaths in central and southern Mozambique (Manhique et al., 2015). More recently, the tropical storm Chedza caused severe flooding in Mozambique in 2015, with more than 20,000 people displaced, and 75 deaths reported in Madagascar (Rapolaki and Reason, 2018).

On inter-annual time scales, rainfall over the Limpopo River Basin, like over much of southern Africa, is strongly impacted on by the El Niño Southern Oscillation (ENSO) (Lindesay, 1988; Nicholson and Kim, 1997; Reason et al, 2000; Washington and Preston, 2006). Typically, El Niño (La Niña) conditions are associated with dry (wet) summers here. However, the relationship between the strength of ENSO events and rainfall over southern Africa is non-linear, i.e. not every El Niño corresponds to dry conditions over the region (e.g. Reason and Jagadheesha, 2005). For example, widespread, below-average dry conditions failed to materialise over southern Africa during the strong 1997/98 El Niño (Lyon and Mason, 2007; Blamey et al., 2018). In contrast, the weaker 1991/92 and 2002/03 El Niño events were linked to severe summer droughts over a large part of southern Africa. Reason and Jagadheesha (2005) showed that the 1997/98 drought was less intense because the Angola low-pressure system (Angola Low) was not anomalously weak, unlike during 1991/92 and 2002/03. Another example of a relatively strong El Niño event for which the Angola Low did not weaken much and hence the expected severe drought did not occur was in 2009/10 (Driver et al., 2018). In that study, experiments with a 0.5° resolution stretched grid global model provided further evidence of the importance of the strength of the Angola Low for summer rainfall variability over the region. The significance of the Angola Low is that it tends to act as the source region for the cloud bands that bring much of the summer rainfall (Harrison, 1984; Hart et al., 2010; Hart et al., 2013).

On a regional scale, sea surface temperature (SST) modes such as the subtropical southern Indian Ocean Dipole (SIOD) (Behera and Yamagata, 2001; Reason, 2001; Reason, 2002) may also influence summer rainfall over the region and can reinforce or oppose the ENSO signal if they occur at the same time. Hoell et al. (2017) presented evidence that when a La Niña and a positive-phase SIOD co-occur, the precipitation anomaly over southern Africa is increased relative to when La Niña co-occurs with a negative-phase SIOD. Climate modes may influence the rainfall of the Limpopo River Basin via inducing anomalies in regional circulation over southern Africa, which then modify the low-level moisture fluxes and uplift. For example, during El Niño, there tend to be anticyclonic circulation anomalies over southern Africa with increased subsidence, with the reverse trend during La Niña. On average, most of the moisture flowing into subtropical southern Africa during summer originates from the western Indian Ocean (D'Abreton and Tyson, 1995), but the tropical southeastern Atlantic can also make important contributions (Cook et al., 2004; Reason et al., 2006; Manhique et al., 2015). Thus, anomalously warm conditions in the tropical southeastern Atlantic (Rouault et al., 2003; Hansingo and Reason, 2009) or in the southwestern Indian Ocean (Walker, 1990; Mason, 1995; Reason, 1998; Reason, 1999; Reason and Mulenga, 1999) during summer have been associated with the increased transport of moist marine air towards southern Africa and hence increased rainfall. Although the relationship between seasonal rainfall patterns and modes of variability over southern Africa has been established to some degree, there has been less focus on how these modes of variability impact on extreme rainfall events over Limpopo, although work has been done on relationships between ENSO and the number of dry spells during the rainy season (Reason and Jagadheesha, 2005). There is also some evidence that the Southern Annular Mode (SAM) may influence rainfall over parts of South Africa during summer (Gillett et al., 2006; Malherbe et al., 2014), although its influence may be stronger in winter (Reason and Rouault, 2002).

To date, there have been very few studies that have investigated variability in daily extreme precipitation events over the Limpopo region. Given its vulnerable and poor rural population, which is largely dependent on rain-fed subsistence agriculture, a better understanding of the nature of rainfall extremes in the Limpopo River Basin is crucial for decision makers, as well as disaster management and seasonal forecasters. To help obtain a better understanding of the relationships between extreme rainfall events over the Limpopo River Basin during summer, this study considers the synoptic weather types associated with the events, and how they may vary through summer. An improved understanding of these events and their variability should then help with their forecasting, as well as with seasonal rainfall outlooks over subtropical southern Africa.

1.1 MERGED PRECIPITATION DATA

Extreme rainfall-producing systems can evolve and dissipate within the span of a few hours, days or weeks, and are difficult to study with monthly averages. Thus, analyses of these events over a longer period, prior to 1996, have been limited by a lack of high-resolution ground-based precipitation data over southern Africa. However, various satellite-derived rainfall products such as the Tropical Rainfall Measuring Mission (TRMM) (Huffman et al., 2009), which has a higher temporal resolution (three-hourly to daily), have been developed based on ground-based observations and using satellite-based algorithms to estimate rainfall (e.g. Huffman et al., 2009; Maidment et al., 2014). Given that many of these products rely on satellites, they tend to only cover the recent period (typically the last 30 years or so), thus making it difficult to investigate the decadal variability of rainfall patterns over southern Africa.

In this study, the daily data of Climate Hazards Infrared Precipitation with Stations (CHIRPS) Version 2 (Funk et al., 2015) is used to identify daily extreme rainfall events over the basin. The CHIRPS dataset combines multiple data, including gauges and satellite imagery, to provide the best estimates of rainfall. Furthermore, CHIRPS was developed to monitor drought conditions over places with complex topography, as well as deep convective precipitation, such as in Ethiopia (Funk et al., 2015), which makes it appropriate for the Limpopo River Basin, which is also dominated by steep topography and convective rainfall. CHIRPS is available at 0.05° (~5 km) spatial resolution on a quasi-global (50 °S to 50 °N) grid for the period 1980 to the near-present, which makes it suitable for this study. Daily rainfall totals were obtained for the region, extending from 0 to 50 °E and 0 to 40 °S, with data falling outside the Limpopo River Basin masked out as depicted in Figure 1.1.

1.2 THE IDENTIFICATION AND RANKING OF EXTREME RAINFALL EVENTS

The method for identifying and ranking the daily extreme rainfall events used here was first proposed by Hart and Grumm (2001) and later modified by Ramos et al. (2014, 2017) for the Iberian Peninsula. The choice of this method is that it takes into consideration both the spatial extent (i.e. an area affected by the event) and the intensity of rainfall over the basin. The 95th percentile is calculated for each grid point. Only grid points with rainfall above 1 mm per day (wet days) for the extended austral summer season (October to April) are considered. Following this, a seven-day running mean (μ) is applied to the 95th percentile for each grid point to smooth the daily climatological noise. The anomalies (N) are then calculated by subtracting the smoothed 95th percentile (μ) values from daily rainfall totals as follows:

$$N = precip_{c,i,j} - \mu_{c,i,j} \quad (1.1)$$

The extreme events are then ranked based on the magnitude (R) of each event given by an index that is obtained after multiplying:

$$R = N \times M \quad (1.2)$$

1) the percentage of grid points that have anomalies (N) above a certain threshold (95th of the long-term climatology) by
2) the mean (M) values of the anomalies over this percentage.

1.3 SYNOPTIC CLASSIFICATION

A key component of this study is to understand the dominant mechanisms through which extreme rainfall is produced in the Limpopo River Basin. As such, a combination of products is used to subjectively identify the type of rainfall-producing system or dominant synoptic setting through which the top 200 extreme events were produced. These include mesoscale convective systems (MCS) and COLs, which were identified subjectively using Gridded Satellite (GridSat-B1) data (Knapp et al., 2011), South African Weather Service (SAWS) synoptic weather maps and National Centers for Environmental Prediction (NCEP)/National Center for Atmospheric Research (NCAR) reanalysis data (Kalnay et al., 1996). Tropical low-pressure systems (depressions, storms and cyclones) were identified from International Best Track Archive for Climate Stewardship (IBTrACS) data (Knapp et al., 2010) and from SAWS synoptic maps. Cloud bands were identified objectively using the output provided by Hart (2012).

To investigate the relationship between the number of events and the seasonal rainfall anomalies, the standardised precipitation anomalies for each year, X_i, for the short seasons (October to December and January to April) and the extended summer season (October to April) were calculated as follows:

$$X_i = \frac{P_i - \bar{P}_i}{\sigma_i} \qquad (1.3)$$

where P_i is the seasonal rainfall, $\bar{P}_i$ is the seasonal rainfall mean for the period 1981 to 2016 for the entire basin, and $\sigma_i$is the standard deviation of seasonal rainfall totals during the same period for the entire basin.

As alluded to in the introduction, summer rainfall in South Africa is modulated by numerous large-scale modes of variability. To assess the potential links between some of the dominant large-scale climate modes of variability and the occurrence of extreme rainfall events in the Limpopo River Basin, the results were correlated with SIOD, ENSO and SAM indices. The Niño 3.4 Index used in this study is based on the Group for High Resolution Sea Surface Temperature (GHRSST) anomalies in the Niño 3.4 box (190 °E to 240 °E; 5 °S to 5 °N). The seasonal (October, November, December/January, February, March April) averages in the Niño 3.4 SST Index above (below) 0.5 °C (-0.5 °C) are defined as El Niño (La Niña), while the averages between -0.5 °C and 0.5 °C are defined as neutral. The Behera and Yamagata (2001) SIOD Index, defined as the difference in SST anomalies between the eastern Indian Ocean (90 °E to 100 °E; 28 °S to 18 °N) and the southwestern Indian Ocean (55 °E to 65° E; 37 °S to 27 °S), was used. The SAM Index used in this study is that of Marshall (2003), which is the monthly mean difference between the mean sea level pressure (SLP) anomalies at six stations close to 40 °S and six stations close to 65 °S.

1.4 SYNOPTIC WEATHER TYPES AND SPATIAL DISTRIBUTION OF EXTREME RAINFALL

In this section, the focus is on all synoptic weather systems linked to extreme rainfall events over the Limpopo River Basin. For the purpose of the analysis, two categories of the rankings are shown: the top 20 and the top 200. Each of the top 200 events was then classified into one of the four main rainfall producing systems: cloud bands, tropical lows (depressions, storms and cyclones), mesoscale convective systems or cut-off lows. Table 1.1 lists a ranking of maximum daily rainfall and the associated rainfall-producing system for each of these top 20 events. Of these 20 events, 45% (nine) were associated with cloud bands, 45% (nine) with tropical lows and 10% (two) were linked to the MCS. This corroborates an earlier finding for tropical systems and their association with widespread extreme multi-day rainfall events over the Limpopo River Basin, based on observed data for the period 1948 to 2011 (Malherbe et al., 2012). For the top 200 events, the proportions remained similar, with 48% of events (96) classified as cloud bands, just over 28% (57) as tropical lows, about 14% (27) as MCS events, and 10% (20) as COLs. It should be noted that the method used in this study identifies and ranks daily precipitation extremes (i.e. heavy rainy days). Several events listed in Table 1.1 (and in the top 200) can thus be linked to a single multi-day event.

Table 1.1. The ranking of the top 20 daily events over the Limpopo River Basin and the accompanying daily maximum rainfall total and synoptic weather type, as determined by analysing SAWS's synoptic charts, IBTrACS data, and outgoing long-wave radiation. The ranking of an event is based on the percentage area of grid points that has rainfall anomalies above the 95th percentile of the long-term climatology multiplied by the mean values of the anomalies over this percentage. It should be noted that several daily events can be linked to a single multi-day event.

Ranking	Event	Rainfall (mm)	Synoptic weather type
1.	20 January 2013	133	Tropical low
2.	5 March 1997	167	Tropical low
3.	24 February 2000	176	Tropical low
4.	9 January 1991	116	Cloud band
5.	27 January 1996	105	Cloud band
6.	17 December 2007	61	Cloud band
7.	23 February 2000	114	Tropical low
8.	6 February 2000	133	Tropical low
9.	28 March 2006	130	MCS
10.	10 February 1996	113	Tropical low
11.	3 March 2006	164	Cloud band
12.	1 December 1989	97	MCS
13.	5 March 1999	122	Tropical low
14.	8 February 1985	188	Cloud band
15.	4 March 2004	169	Tropical low
16.	31 January 1981	129	Cloud band
17.	22 March 1984	66	Cloud band
18.	19 April 1986	66	Cloud band
19.	17 January 2000	121	Tropical low
20.	18 February 1991	125	Cloud band

Figure 1.2 shows spatial rainfall distributions and the synoptic system linked to the top 20 events over the entire basin. The transition zone between the steep topographical areas over northeastern South Africa and the floodplains in southeastern Mozambique generally received higher amounts of rainfall compared to the northern and western parts of the basin (southern Zimbabwe and southeastern Botswana, respectively). Heavy rainfall linked to tropical lows (depressions, storms and cyclones) was primarily confined to the eastern parts of the basin with the maximum amounts occurring over the steep topographic regions (Figure 1.2). No discernible difference could be found with regard to the total spatial coverage of rainfall between the different rainfall-producing systems in the top 20 events. Furthermore, the maximum daily rainfall received at a particular point in the Limpopo River Basin varies from one event to another, and ranges from 61 mm (event ranked number 6) to 188 mm (event ranked number 14).

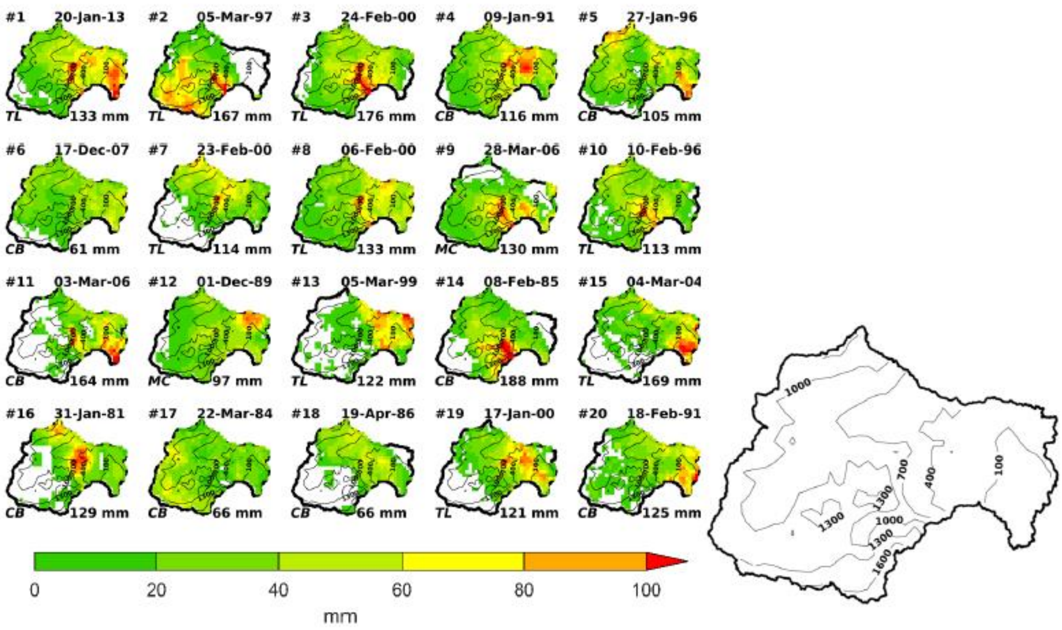

Figure 1.2: Daily rainfall (shaded; units are in mm) of the top 20 ranked extreme rainfall events over the Limpopo River Basin. The contours in the panels represent the local topography, while for clarity, a zoomed topography map is inserted in the bottom right. Symbols CB, TL and MC in the bottom left corner of each panel denote the different rainfall mechanism associated with each event (CB = cloud band; TL= tropical low; MC = mesoscale convective system). The maximum rainfall during each event is given in the bottom right-hand corner.

1.5 MONTHLY DISTRIBUTION OF HEAVY RAINFALL EVENTS AND SYNOPTIC WEATHER TYPES

Figure 1.3a shows the monthly distribution of extreme events in the two categories, illustrating that, for the top 20 extreme event, there is an increase from December through to a maximum in February/March and then a sharp decrease in April. For the top 200 case, there are substantial numbers in all months from October to April, but with an obvious increase in January and a maximum in March. Thus, the second half of summer tends to show more events for both categories. The monthly breakdown of each rainfall-producing type for the top 200 extreme events is provided in Figure 1.3b. Apart from the COLs, the seasonal cycle of each weather system that contributes to extreme rainfall is similar to that described above, with the largest number of events occurring during the late summer months (January to March), and the smallest number of events occurring during the early summer months (October to December). The COL timing in Figure 1.3b is consistent with Singleton and Reason (2007b), who found that these systems are most common over subtropical southern Africa in the transition seasons.

Over the seven-month period, the number of cloud band-related events per month in the top 200 (Figure 1.3b) ranged from nine to twenty, increasing from a minimum in October to a maximum in February, with a sharp decline in April, broadly consistent with Hart et al. (2013). The number of tropical lows also generally increases through the summer (from November), but has a later maximum (March) than cloud bands, and again decreases rapidly in April. For MCS events, the monthly frequency is variable through the summer, but with a peak in January. However, it is not uncommon for MCS events to be embedded within cloud bands. The analysis may thus underestimate the role of such systems in extreme rainfall events in the region.

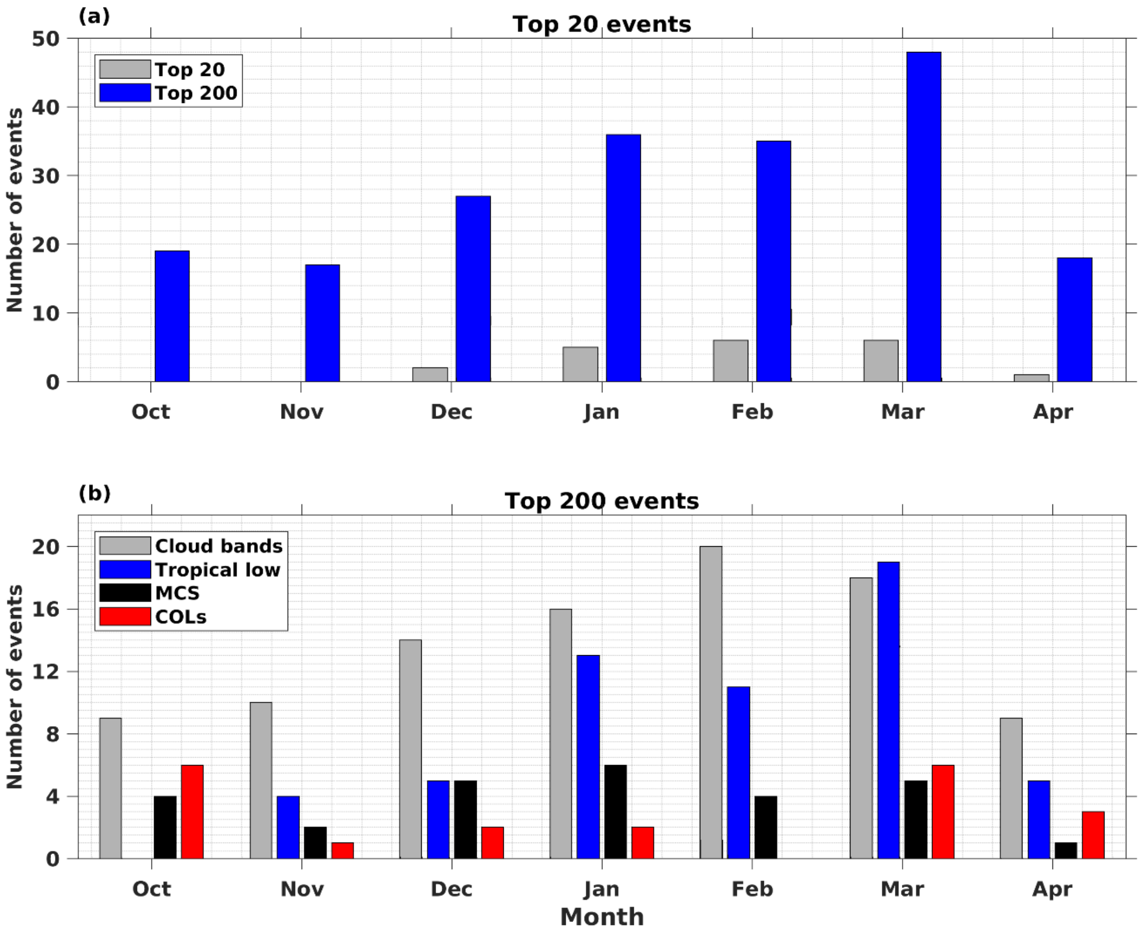

Figure 1.3: (a) The monthly distribution of extreme rainfall events over the Limpopo River Basin during the austral summer months for the period 1981 to 2016. The top 20 events are represented by grey bars, while the top 200 are represented by blue bars.
(b) Monthly distribution of rainfall-producing systems that lead to extreme rainfall over Limpopo for the top 200 heavy rainfall events (cloud bands are in grey, tropical lows are in blue, MCS events are in black and COLs are in red).

1.6 SUMMARY

This section set out to identify and classify rainfall-producing systems linked to extreme rainfall events over the Limpopo River Basin in southeastern South Africa during the period 1981 to 2016. Long-term studies of extreme weather events over southern Africa are limited by a lack of high spatial and temporal observation data. However, satellite-derived rainfall estimates with a higher temporal and spatial coverage have been invaluable in providing “observations” in data-poor regions. In this study, CHIRPS rainfall data was used to identify extreme rainfall events over the Limpopo River Basin.

It was found that the spatial distribution of rainfall associated with extreme rainfall events is not uniform over the basin, with a bias of more extreme rainfall towards the eastern half of the region. This east-west gradient in extreme rainfall events is consistent with the annual and seasonal mean rainfall patterns (Mosase and Ahiablame, 2018). An obvious characteristic is the spatial pattern of the rainfall maximum over areas with a steep topographic gradient between the mountainous (e.g. the Drakensberg Mountain) areas of northeastern South Africa, where the altitude rises above 1,300 m, and the Mozambican floodplains.

Although this study does not specifically focus on the topographic effects on rainfall over the Limpopo River Basin, the local topography is known to have important consequences for rainfall over southern Africa (Dedekind et al., 2016). Furthermore, there is evidence that the coastal mountains of eastern and southern South Africa have resulted in extreme rainfall during COL and MCS events (Singleton and Reason, 2006; Singleton and Reason, 2007a; Blamey and Reason, 2009). East of the topography in the Limpopo River Basin, the Mozambican floodplains also tend to receive high amounts of rainfall, likely due to their immediate proximity to the relatively warm waters of the Mozambican Channel, where tropical storms, and occasionally tropical cyclones, develop. Such storms, when they make landfall on the mainland, tend to do so either near the far eastern Limpopo River Basin or a bit further north along the Mozambican coast. Their intensity tends to weaken substantially as they track further inland. The eastern Limpopo River Basin is thus more likely to receive more rainfall from these tropical storms than the rest of the Limpopo River Basin.

The classification of the top 200 extreme rainfall events suggests that most events over the basin are associated with cloud bands (48%) and tropical lows (28%), with MCS events (14%) and mid-to-upper level COLs (10%) making up the remaining quarter. The fact that most events in the top 200 are associated with cloud bands is in agreement with previous studies (Harrison, 1984; Reason et al., 2006; Hart et al., 2010; Hart et al., 2013; Manhique et al., 2011), which further indicates their importance for rainfall over southern Africa. The monthly distribution of COLs over the basin agrees with the findings of Taljaard (1985), Singleton and Reason (2007b) and Favre et al. (2012), in which they showed that COLs over southern Africa occur mostly during transition seasons and that they are important contributors to early and late summer rainfall.

Monthly distribution of the events showed that the late summer months (January to March) had the highest number of top 200 events. Approximately 60% of these extreme events occurred during January, February and March, a time when convective processes dominate over the southern African summer rainfall region (Tadross et al., 2005). Blamey et al. (2017) found marked differences between the early and late summer over northern South Africa in severe convective environmental characteristics such as convective available potential energy and deep-layer wind shear. Mason and Jury (1997) demonstrated that, during late summer (January to March), tropical convection migrates southward to about 20 °S over the subtropics, linked to the formation of the cloud bands, which creates favourable conditions for rainfall over the Limpopo River Basin. Dyson et al. (2015) indicated that the atmospheric conditions over the northeastern parts of South Africa evolve from having an extratropical nature in early summer to having a more tropical nature in late summer.

CHAPTER 2: INFLUENCE OF THE BOTSWANA HIGH ON RAINFALL OVER THE LIMPOPO RIVER BASIN

The Botswana High is a mid-level anticyclone that develops over tropical southern Africa in austral spring as part of the dynamic response to heavy precipitation over the Congo Basin. During summer, it strengthens and moves south so that, by February, it is centred over central Namibia and western Botswana. Figure 2.1 shows its position relative to other important circulation features over southern Africa in summer. As yet, the impact of variability in this circulation system on rainfall over the region is not well understood.

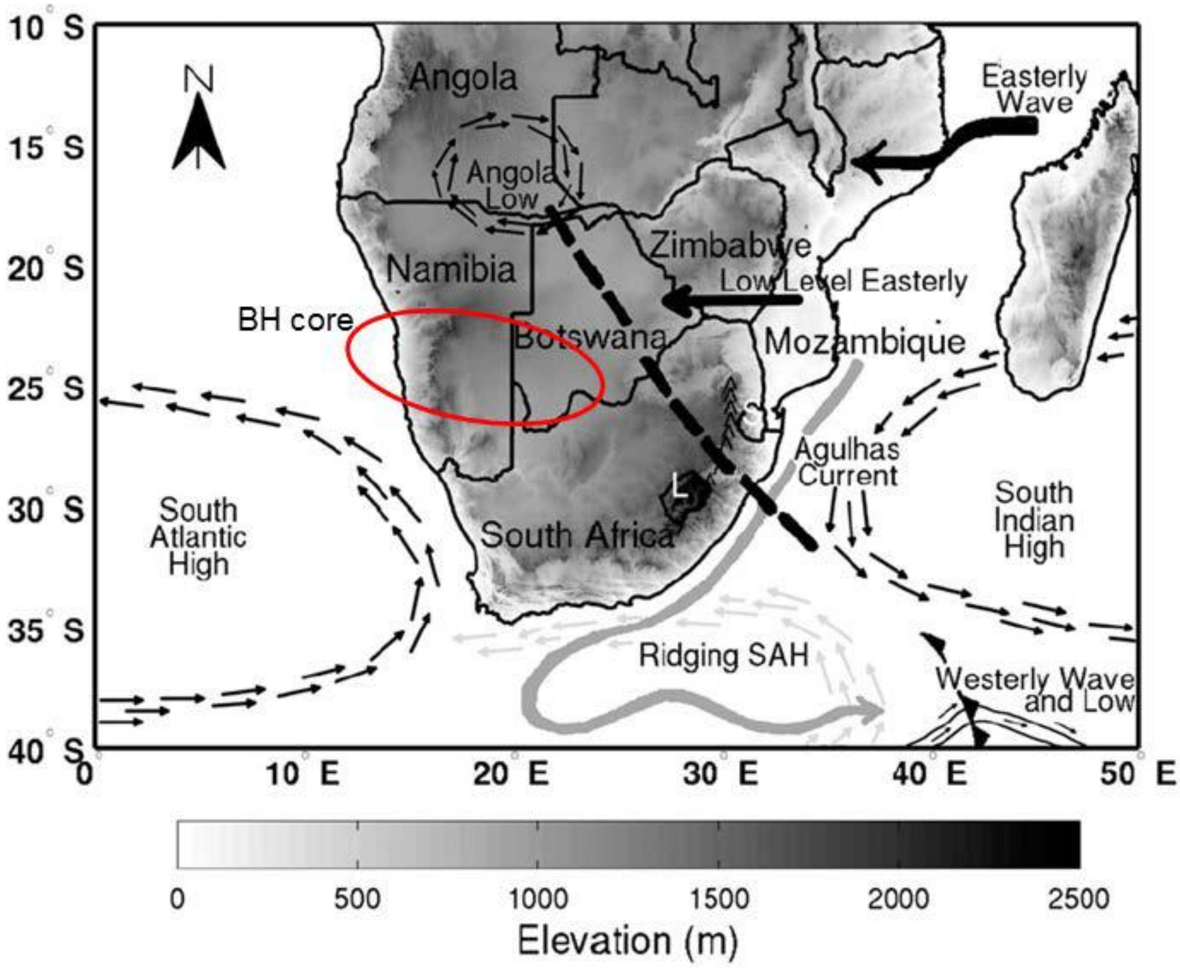

Figure 2.1: The core (red ellipse) of the Botswana High at 500 hPa relative to other important circulation features over southern Africa in summer. The black dashed line shows a typical tropical temperate trough that stretches from the near-surface Angola Low in the southeastern to the southwestern Indian Ocean (after Reason, 2019).

An index for the Botswana High was created by spatially averaging the 500 hPa NCEP reanalysis geopotential height over the box 19-23 ^{o}S, 16-21 ^{o}E for the period 1979 to 2015. Data prior to the satellite era (pre-1979) was not included due to an obvious shift in values at this time. Figure 2.2 shows this time series plotted along with a spatially averaged rainfall time series over the region (15-25 ^{o}S, 17-40 ^{o}E). The two series are correlated at $r = -0.74$ (significant at 99.9%), which is greater than the correlation of this rainfall index with ENSO.

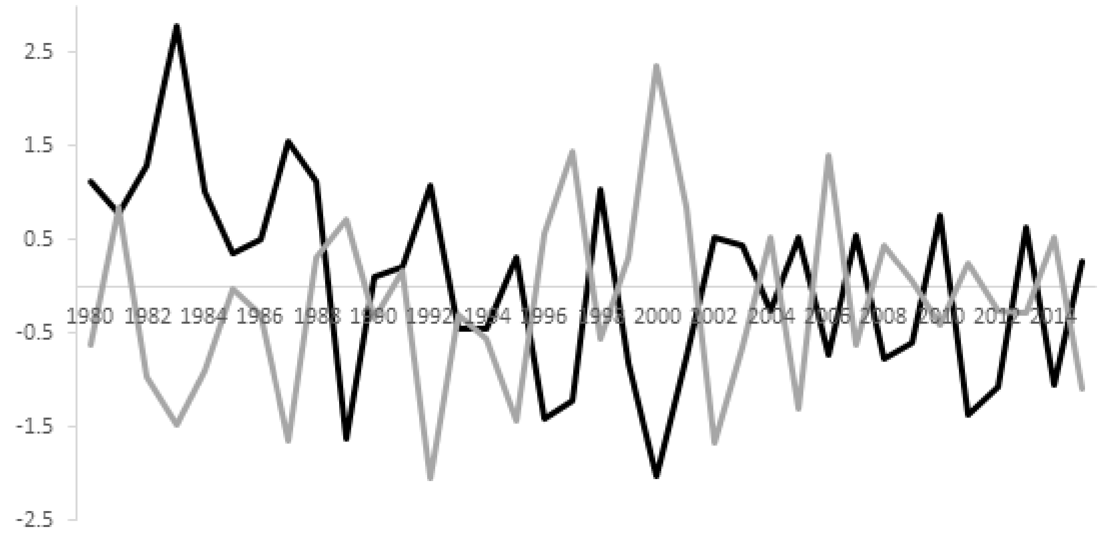

Figure 2.2: *Standardised anomalies of the Botswana High Index (black) and summer rainfall over southern Africa*

The impact of anomalies in the Botswana High on summer rainfall was investigated using composites for summers that are neutral with respect to ENSO and which had large departures from the mean in the strength of the Botswana High Index. Figure 2.3 shows anomalies in rainfall and 850 hPa zonal wind during such summers with an anomalously weak Botswana High.

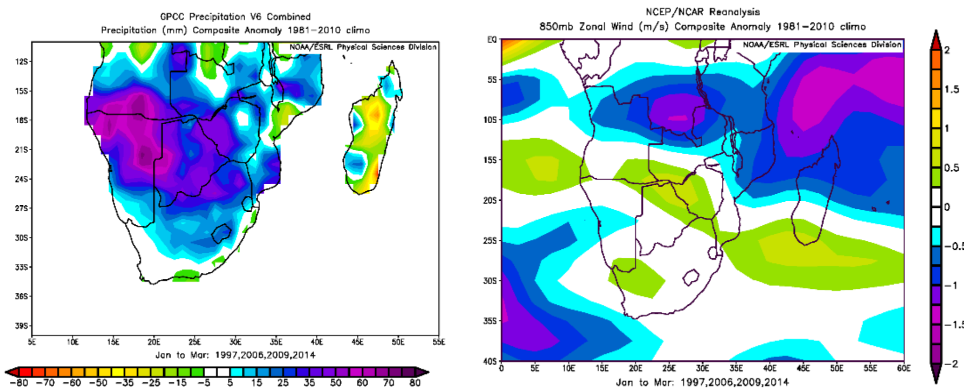

Figure 2.3: *Anomalies in rainfall (mm/month) and 850 hPa zonal wind (m/s) for neutral summers with an anomalously weak Botswana High*

It is clear that the entire Limpopo River Basin, as well as large parts of Namibia, Angola and central South Africa, receive above-average rainfall when the Botswana High is anomalously weak. These increases in rainfall are associated with increased westerly winds over the tropical southeastern Atlantic, which feed more moisture into the Angola Low, and hence strengthen the TTT cloud bands. Increased easterlies are also seen over the tropical western Indian Ocean, thereby feeding in more moist marine air from that source towards southern Africa. Roughly the opposite patterns are seen for those neutral summers, with an anomalously strong Botswana High (Figure 2.4), although the magnitude of the drier conditions is not as large as that seen in Figure 2.3 for the summers of the weak Botswana High. The area with the strongest anomalies has shifted more towards Botswana and central Zimbabwe. Weaker westerlies that feed into the Angola Low from the tropical southeastern Atlantic and easterlies from the western Indian Ocean are evident.

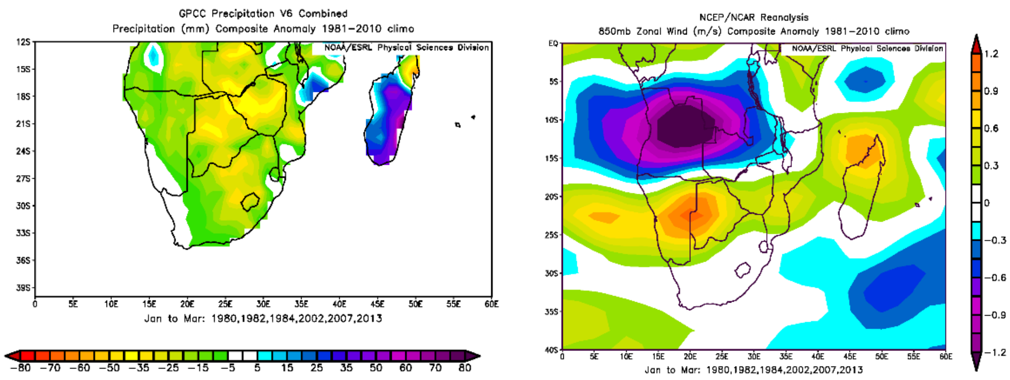

Figure 2.4: Anomalies in rainfall (mm/month) and 850 hPa zonal wind (m/s) for neutral summers with an anomalously strong Botswana High

In addition to seasonal totals, it is of great interest to assess relationships with synoptic dry spells during the summer since the number of these that occur is important for water resource managers, farmers and other user groups. A dry spell is defined as a pentad (five days) that receives less than 1 mm of rainfall per day on average. Using Global Precipitation Climatology Project (GPCP) daily rainfall data from 1997 to 2012, Figure 2.5 shows the mean summer frequency of dry spells.

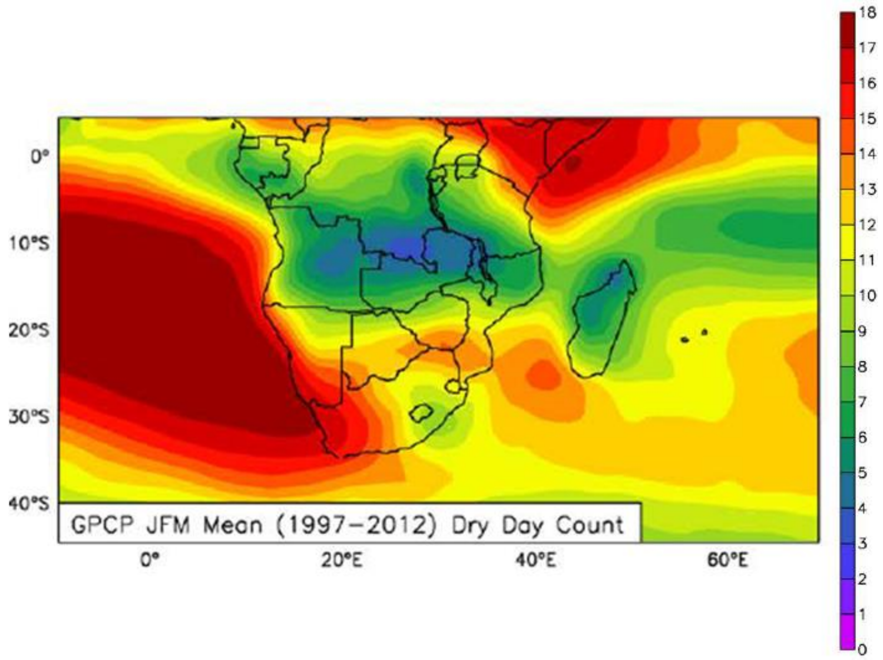

Figure 2.5: The mean frequency of January, February and March dry spells computed from GPCP data

As expected, the smallest number of dry spells occurs over the Intertropical Convergence Zone (ITCZ) in northern Madagascar, northern Mozambique and its meridional arm through Zambia and the eastern Congo Basin, as well as over the confluence zone between the Angola Low and this arm. Almost the entire summer is dry along the west coast of South Africa and Namibia, and a strong gradient exists between these semi-arid or arid areas across the land to the east coast of South Africa, as well as north towards the confluence zone.

Prominent across the subcontinent from southern Mozambique to southwestern Botswana/southern Namibia is the so-called “drought corridor” of the Limpopo region identified by Usman and Reason (2004) as one where 60-100% of the 21 summers analysed by these authors experienced dry spells for at least half of the summer rainy season. The northern South African region falls completely within this drought corridor, as does most of the central South African region. The time series of anomalies in dry spell frequencies for the northern and central region are shown in Figure 2.6, while Table 2.1 lists the correlations between these anomalies and the Botswana High Index. Statistically significant correlations exist for both areas, with the strongest relationship existing for the northern South African region. In general, the relationship between the Botswana High Index and the dry spell frequency is stronger than that between ENSO and the dry spell frequency.

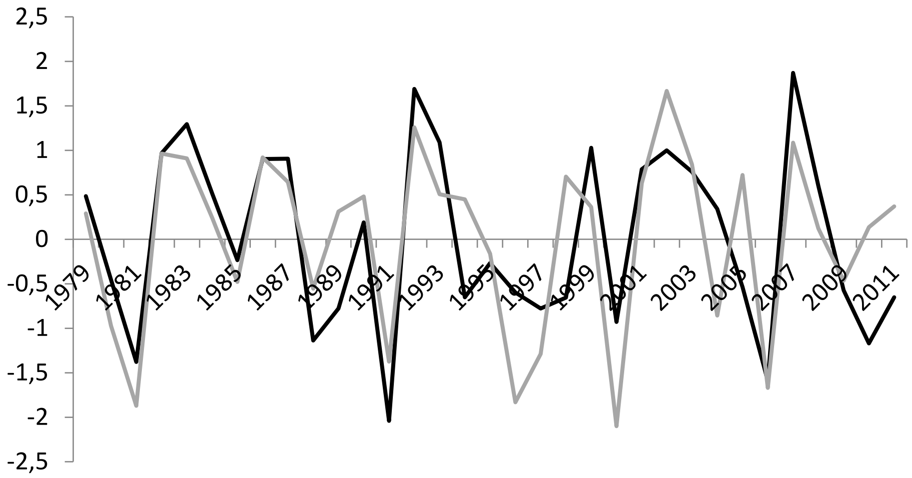

Figure 2.6: Anomalies in dry spell frequency for northern South Africa (grey) and central South Africa (black)

Table 2.1: Correlations with anomalies in January, February and March dry spell frequency (bold italics indicate statistical significance at 95%

	Central South Africa	Northern South Africa
Nino 3.4	0.21	***0.41***
Botswana High	***0.35***	***0.48***

It is clear from figures 2.1 to 2.6 and Table 2.1 that a strong relationship exists between the Botswana High and summer rainfall over the Limpopo River Basin (as well as a larger region of southern Africa). Thus, summers with an anomalously strong (weak) Botswana High tend to have more (less) summer rainfall and a reduced (increased) frequency of synoptic dry spells during this season. The mechanisms involve changes in low-level wind (and hence moisture transport) from the tropical southeastern Atlantic and western Indian Ocean, as well as in the amount of subsidence over the subcontinent. Modelling studies are, however, required to further explore the robustness of these relationships.

In addition to the interannual variability described above, there is substantial decadal-multidecadal variability in the Botswana High. Since it is well known that summer rainfall over southern Africa may experience a roughly 18- to 19-year cycle in rainfall (Tyson et al., 1975), it is of interest to see whether this may be related to low-frequency variability in the Botswana High. Figure 2.7 plots the time series of the Botswana High Index and summer rainfall averaged over 15-40 ^oE, 15-30 ^oS.

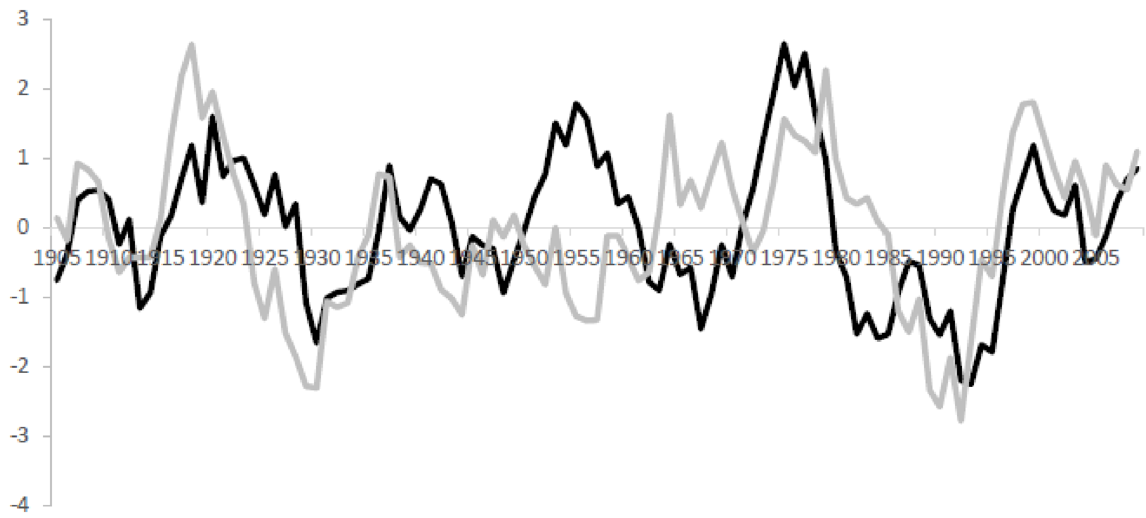

Figure 2.7: Time series of southern African rainfall (black) and the Botswana High for summer after smoothing with a seven-year running mean

The two series are correlated at r = 0.49 (significant at 99%), which increases to r = 0.64 for the 1960-2011 period. It is clear from Figure 2.7 that there are obvious wet (approximately late-1990s to late-2000s, 1970s, 1950s and 1920s) and dry (approximately 1980s to early 1990s, 1960s and 1930s) periods through the record of roughly decadal duration, although some of these epochs are shorter and of a different intensity than others. For example, the 1972-1980 period stands out as the wettest, but this spell is somewhat shorter in duration than the next wettest spell (1950-1962) or the 1916-1928 wet period. The most obvious dry period is 1981-1994. This was somewhat longer and more intense than the 1963-1971 dry spell. The period from 1929 to 1949 contains two relatively intense dry spells, punctuated by two relatively short wet spells. These variations in the lengths of the individual dry and wet periods suggest that identifying a single cause may be difficult and that there may rather be more than one contributing factor to their existence. It also suggests that emphasis on the period of low-frequency variability as one of 18 years, such as in Tyson et al. (1975, 2002) may over-simplify the nature of the rainfall signal. In fact, a spectral analysis of the time series reveals several peaks that are significant at 95%; namely 2.3 and 3.9 years on the interannual scale and two decadal peaks at 10.9 and 19.6 years. A wavelet analysis (not shown) indicates strong power at a period close to 20 years during 1948 to 1998 and at a period close to 11 years from about 1968 to 2002. In addition to these periods of strong decadal variability on the records, there are periods of strong interannual variability (a two- to four-year period), particularly during about 1915-1930 and about 1968-2001.

As yet, there is no definitive explanation for the driver of this low-frequency signal in rainfall, although a number of potential explanations have been proposed. These include changes in regional SST (Mason, 1990; Mason, 1995; Reason and Mulenga, 1999), modulation of tidal forcing by the 18.6-year lunar nodal cycle/SAM interactions (Malherbe et al., 2014), ENSO-like decadal variability (Reason and Rouault, 2002), and the Pacific Decadal Oscillation and the Interdecadal Pacific Oscillation (Malherbe et al., 2016). It is therefore natural to investigate linkages between low-frequency variability in the Botswana High and related circulation patterns, and the decadal rainfall signals. Below, circulation patterns associated with low-frequency variability are considered.

To highlight circulation patterns that may be behind the decadal rainfall variability and to avoid the contamination of signals by any underlying trend, figures 2.8 to 2.12 plot differences in rainfall, circulation and regional temperature between the wet and dry epochs implied in Figure 2.7.

These are 1972-1980 (wet) minus 1981-1994 (dry), 1950-1962 (wet) minus 1963-1971 (dry), and 1916-1928 (wet) minus 1929-1949 (dry).

The first two epoch differences (Figure 2.8) show large areas of relatively wetter conditions (1-2 mm per day or about 120-240 mm over the December, January, February and March season) over many parts of southeastern Africa. For the 1916-1928 minus 1929-1949 epoch, there are smaller areas of wetter conditions that extend west from central Mozambique towards northern Namibia/southern Angola, but show a smaller increase in rainfall further south.

While Figure 2.9 shows that each epoch difference is characterised by a weaker and southward-shifted Botswana High, consistent with wetter conditions, there appear to be two cases. In the most recent epoch difference (Figure 2.9a), the changes in the Botswana High seem to be linked to a broader weakening of geopotential height across most of the southern hemisphere tropics. This difference pattern may reflect the occurrence of a strong protracted La Niña during the mid-1970s and two strong El Niño events during the 1980s. On the other hand, for the last two epoch differences (Figure 2.9b and 2.9c), the changes in the Botswana High appear to be more closely linked to those over the midlatitude southern Atlantic and southern Indian oceans rather than to any coherent pattern in the tropics. A weaker or southward-shifted Botswana High implies reduced mid-tropospheric subsidence over the region and is hence consistent with increased rainfall.

Figure 2.10 plots epoch differences in omega at the 500 hPa level, with negative differences implying relative uplift and positive differences implying relative sinking. For the two most recent epoch differences, there are large negative values over southern Angola, extending east over the southern Congo Basin, which are typical source regions for the cloud bands that bring much of the summer rainfall. Weaker negative differences are present over the Botswana High region and over many other areas in southern Africa, consistent with the increased rainfall. For the 1916-1928 minus 1929-1949 case, there are weak negative differences over much of the region, but relatively larger values over central and northern Mozambique near where the rainfall differences are the greatest.

Epoch differences in low-level winds (Figure 2.11) also show some important commonalities. In general, the southwestern Indian Ocean is an important moisture source for southern Africa (D'Abreton and Tyson, 1995; Reason et al., 2006), although the tropical southeastern Atlantic can also make a substantial contribution during synoptic or intraseasonal wet spells in the summer (Cook et al., 2004). Reason (2019) showed evidence that, averaged over the summer, there are two main low-level moisture sources from the western Indian Ocean; the first represents the northeast monsoonal flow into southern Tanzania and northern Mozambique, which extends into the meridional arm of the ITCZ through western Tanzania/eastern Congo, and the second is the easterly flow into southern Mozambique and northeastern South Africa associated with the Mozambican Channel trough.

For each epoch difference plot, there are easterly anomalies in the western tropical Indian Ocean, indicating a stronger northeast monsoon and increased moisture transported from this ocean towards Tanzania and northern Mozambique. The two most recent epoch differences (figures 2.11a and 2.11b) also show easterly anomalies in the northern Mozambican Channel, implying reduced flux of moisture away from northern Mozambique by the mean northwesterly flow towards northern Madagascar, thus increasing that available for storm development over the southern African mainland. Further south, there are areas of increased easterly flow towards the south coast of Mozambique and the east coast of South Africa, although the location differs in each epoch difference. Nevertheless, these enhanced easterlies also imply increased moisture transported towards southeastern Africa from the subtropical southwestern Indian Ocean; and are hence also favourable for wetter conditions over subtropical southern Africa.

Each epoch difference also shows westerly differences over parts of the tropical southeastern Atlantic, implying increased moisture transported from this ocean region towards the Angola Low where the cloud bands typically originate. Hence, these anomalies are also favourable for increased rainfall over the subcontinent.

To assess whether any surface temperature differences are associated with differences in rainfall, Figure 2.12 plots skin temperature in each case. In general, there are areas of relative cooling in each case near where there are rainfall differences consistent with increased cloud cover and convection over the landmass in the wetter epochs. The implied SST epoch differences show some areas of weak warming in the southwestern Indian Ocean, and east of Madagascar, as well as in the southern Mozambican Channel, which are all regions that are known to be linked with increased rainfall over southeastern Africa (e.g. Mason, 1995; Reason and Mulenga, 1999; Reason, 2002). The first and last epoch difference (figures 2.12a and 2.12c) also show a cooler SST in the eastern Pacific, which bears some resemblance to a broad-scale La Niña or negative interdecadal Pacific oscillation pattern, as well as La Niña-like cooling in the tropical Indian Ocean. La Niña-like SST conditions are often associated with increased summer rainfall over southern Africa (Lindesay, 1988; Reason et al., 2000; Allan et al., 2003; Reason and Jagadheesha, 2005; Washington and Preston, 2006). In the Indian Ocean, the second epoch difference shows a pattern similar to the decadal SST mode found by Ansell et al. (2000). In the tropical southeastern Atlantic, each epoch difference also shows areas of warming off the coast of Angola/northern Namibia, which has previously been associated with wet summers over parts of southern Africa (Hirst and Hasternrath, 1983; Rouault et al., 2003; Hansingo and Reason, 2009).

2.1 SUMMARY AND DISCUSSION

The Botswana High is a mid-level anticyclone that forms in the austral spring over western tropical southern Africa and then moves south and strengthens during the summer so that its core region is located over central Namibia and western Botswana from December through to March. Previous work has shown a strong seasonal and interannual relationship between this high-pressure system and summer rainfall over the sub-continent (Driver and Reason, 2017). However, lower-frequency variability in the Botswana High has not been studied before. Hence, given the well-known existence of decadal to multidecadal rainfall variability over southern Africa (e.g. Tyson et al., 1975; Reason and Rouault, 2002; Malherbe et al., 2016), this study has also investigated decadal variability in the Botswana High and its relationships with regional rainfall, temperature and circulation using 20th-century NCEP reanalysis data.

Using the smoothed rainfall series in Figure 2.7, the wetter epochs are characterised by a weaker and southward-shifted Botswana High and reduced subsidence over southern Africa. There are also low-level easterly wind anomalies over the southwestern Indian Ocean and westerly anomalies over the tropical southeastern Atlantic Ocean, implying increased moisture flux towards southern Africa consistent with increased rainfall. Wetter epochs are also associated with reduced surface temperature over much of the land mass, consistent with increased cloud cover. There is also weak warming present in parts of the southwestern Indian Ocean and the Mozambican Channel, consistent with previous work that has found relationships between SST in this region and summer rainfall (e.g. Walker, 1990; Mason, 1995; Reason and Mulenga, 1999). The 1972-1980 (wet) minus 1981-1994 (dry) epoch difference, as well as that for 1916-1928 (wet) minus 1929-1949 (dry) are characterised by cooling in the eastern and central Pacific and in the tropical Indian Ocean, reminiscent of a broad-scale La Niña or negative interdecadal Pacific oscillation SST pattern.

The results presented here suggest that decadal variability in the Botswana High is an important feature of this circulation system and may have a strong relationship with the well-known decadal variability in southern African summer rainfall. Linkages with regional surface temperature were also found in this study. It is important to better understand this low-frequency variability since it is likely to sometimes oppose and, at other times, reinforce trends in regional rainfall and temperature associated with global warming.

As a result, until this anthropogenic forcing strongly dominates the natural variability signals, climate change signals over the region could, to some extent, be obscured in the near-term, posing challenges for the appropriate attribution and detection of climate change.

a)

b)

c)

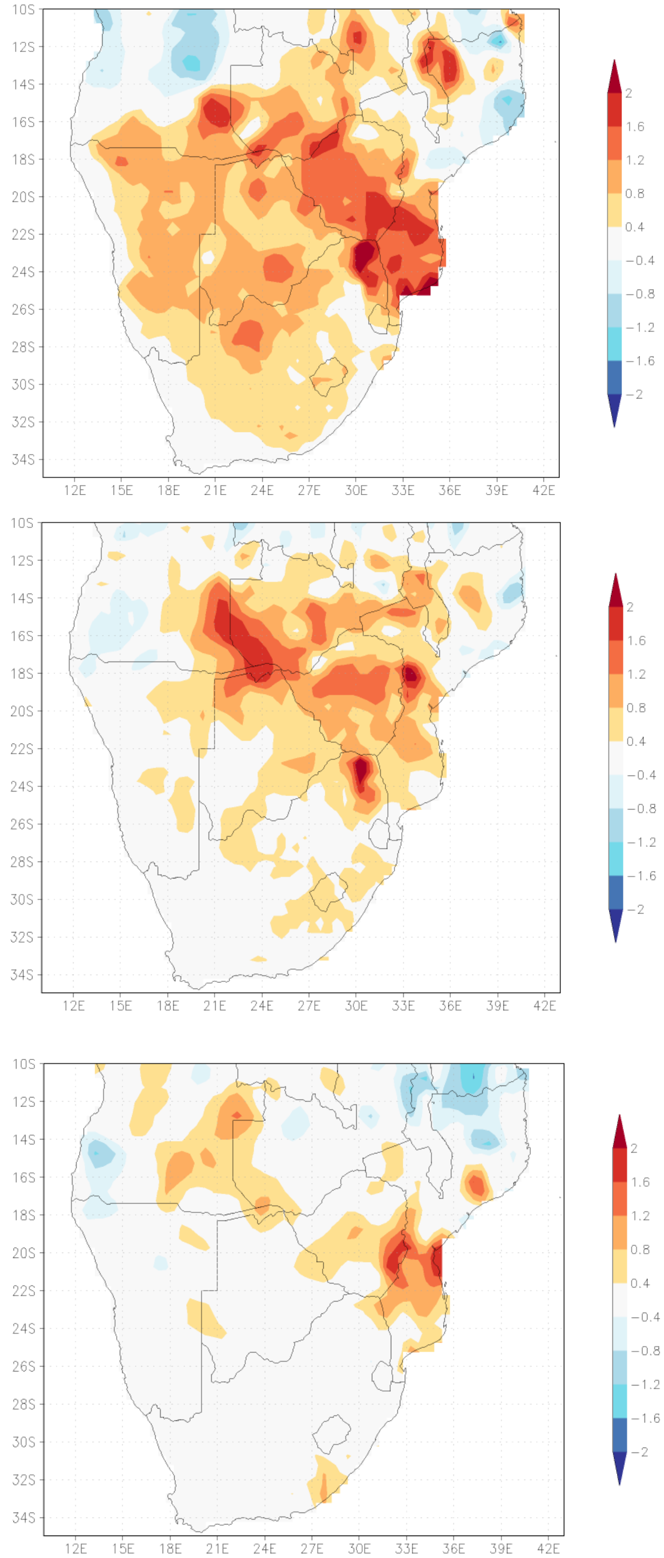

Figure 2.8: *Wet minus dry epoch differences in December to March rainfall (mm/day) for: (a) 1972-1980 minus 1981-1994; (b) 1950-1962 minus 1963-1971; and (c) 1916-1928 minus 1929-1949*

a)

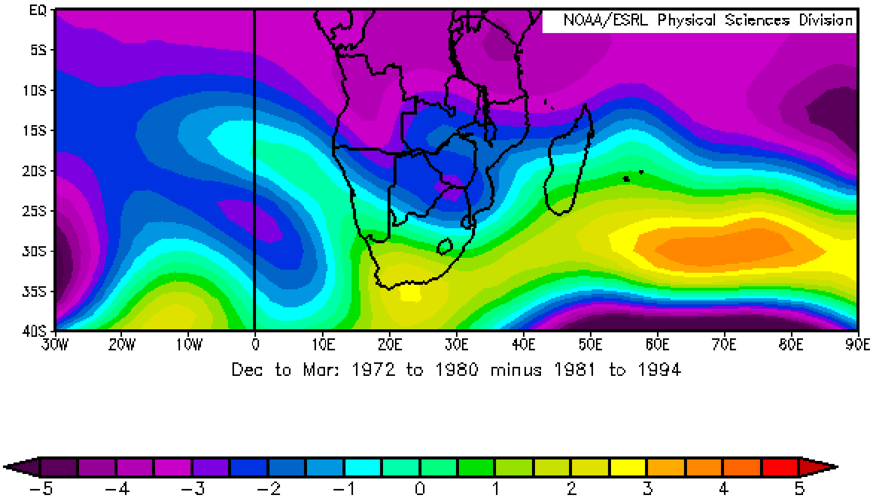

b)

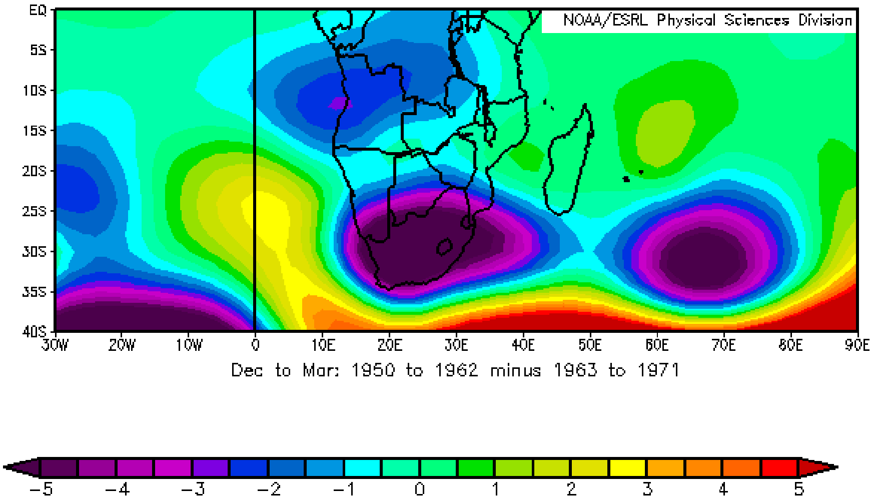

c)

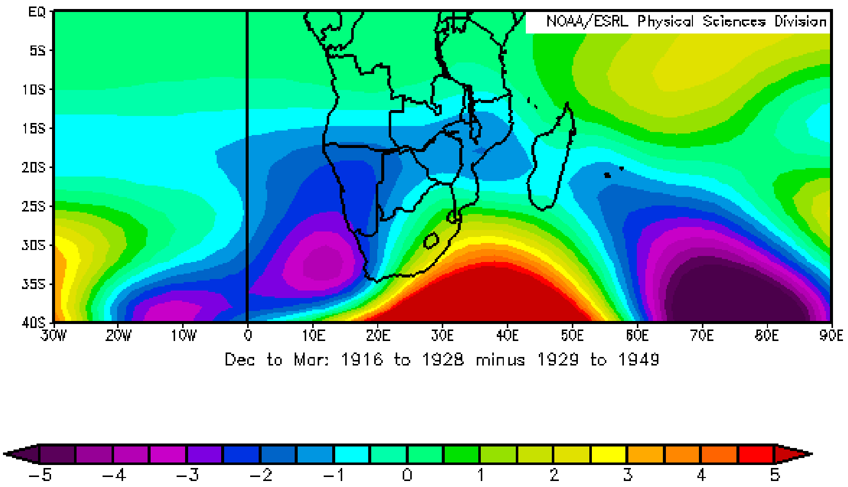

Figure 2.9: *As for Figure 2.8, except epoch differences in December to March 500 hPa geopotential height (m) from 20th-century reanalyses*

a)

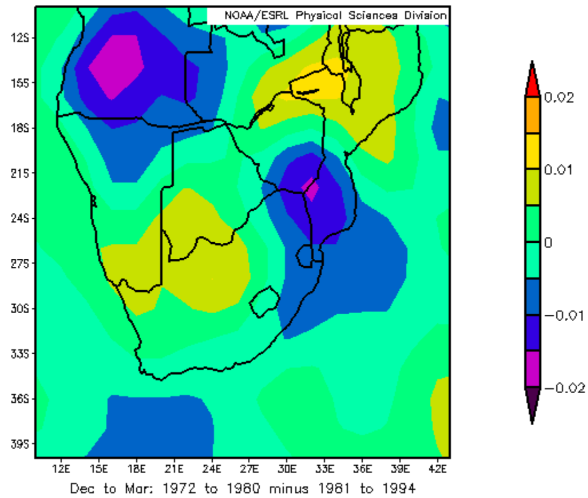

b)

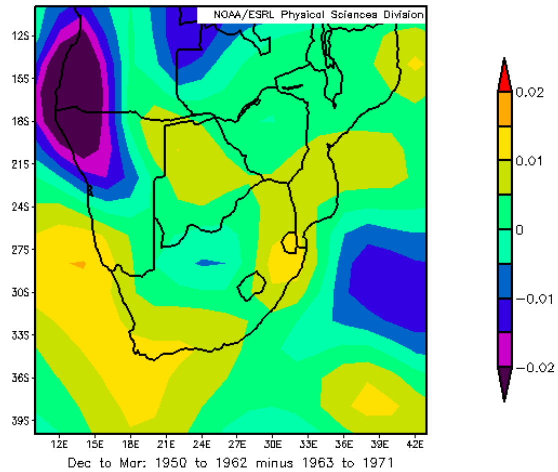

c)

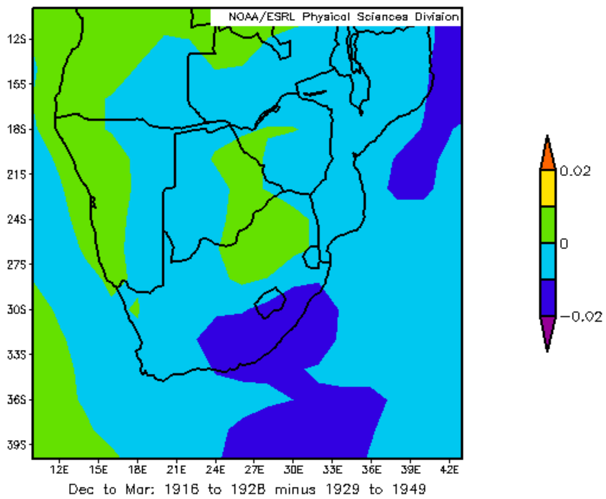

Figure 2.10: As for Figure 2.8, except epoch differences in December to March 500 hPa omega (Pa s^{-1}) from 20th-century reanalyses

a)

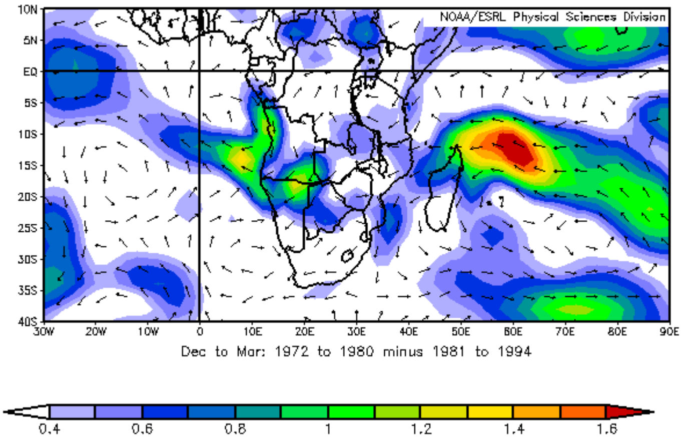

b)

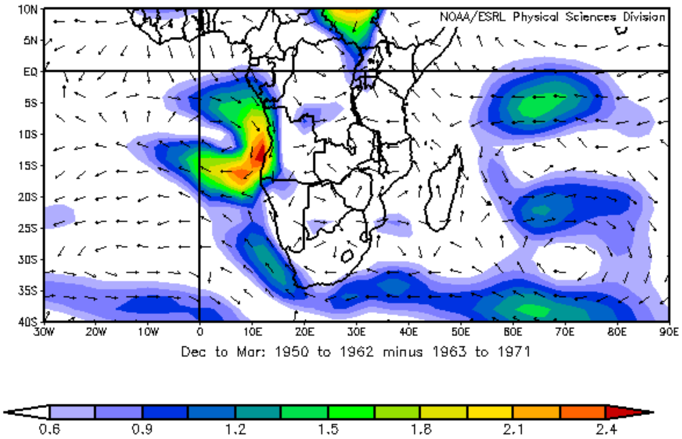

c)

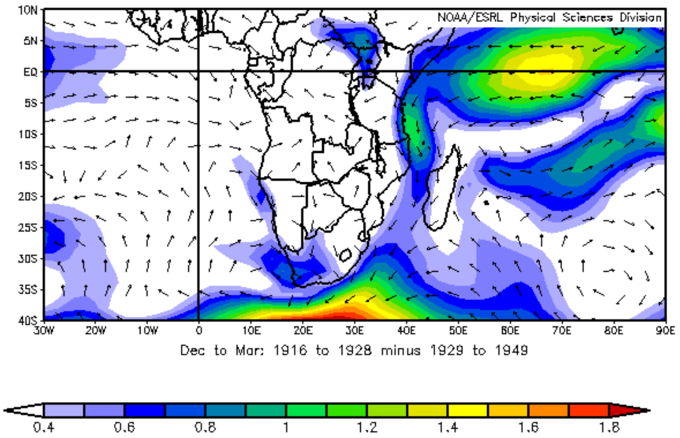

Figure 2.11: As for Figure 2.8, except epoch differences in December to March 850 hPa wind (ms^{-1}) from 20th-century reanalyses

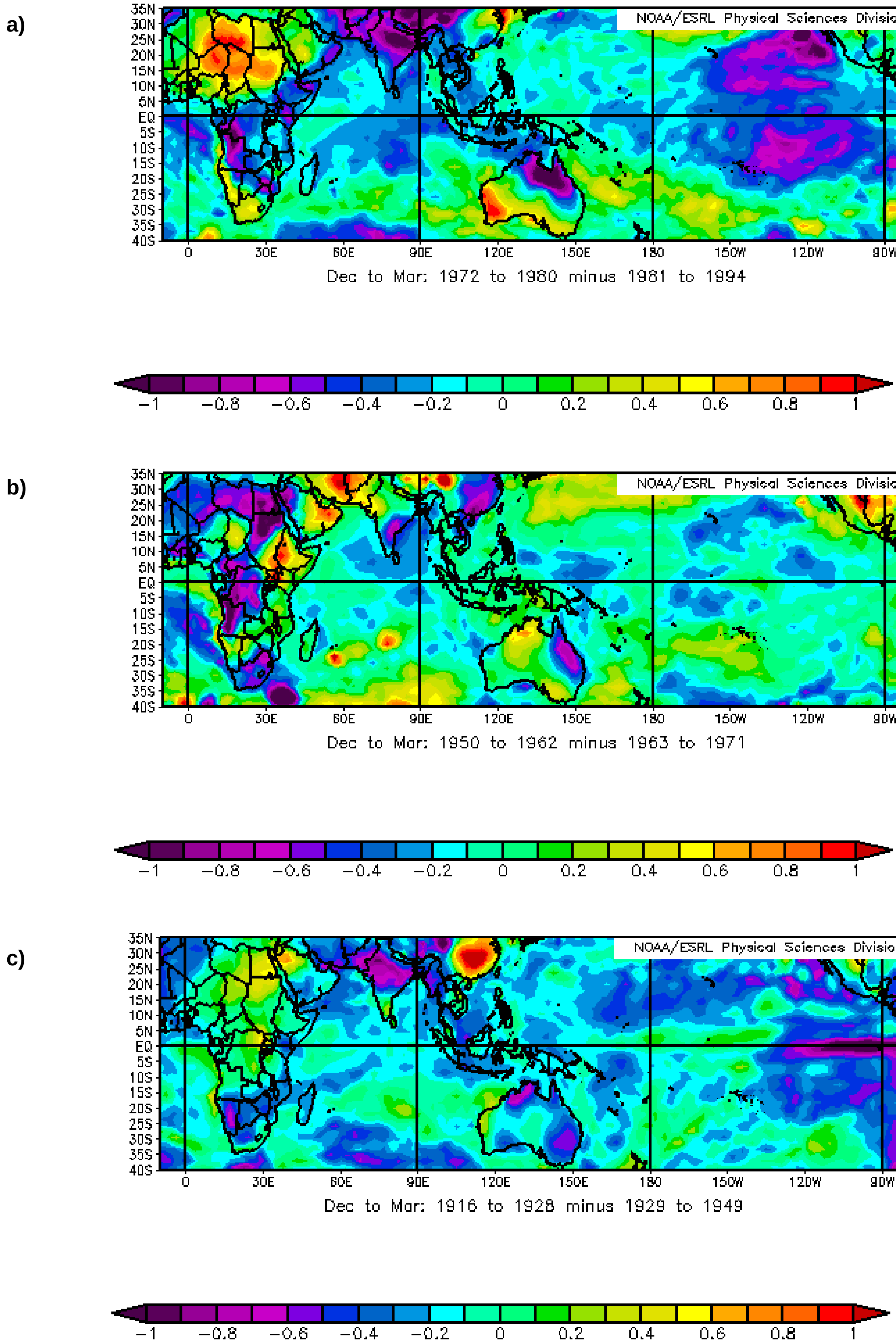

Figure 2.12: As for Figure 2.8, except epoch differences in December to March surface skin temperature (°C) from 20th-century reanalyses

CHAPTER 3: OTHER INFORMATION

The work reported on here has been published in the following international refereed literature:

- RAPOLAKI R, BLAMEY RC, HERMES J and REASON CJC (2019) A classification of synoptic weather patterns linked to extreme rainfall over the Limpopo River basin in southern Africa. Climate Dynamics **53** 2265–2279. http://doi.org/10.1007/s00382-019-04829-7.
- REASON CJC (2019) Low frequency variability in the Botswana High and southern African regional climate. Theoretical Applied Climatology **137** 1321–1334. http://doi.org/10.1007/s00704-018-2661-8.

In addition, collaboration with Portuguese scientists as a result of the IMDROFLOOD project has led to the following papers on Western Cape rainfall variability and the recent "Day Zero" drought:

- BLAMEY R, RAMOS A, TRIGO R and REASON CJC (2018) The influence of atmospheric rivers over the south Atlantic on winter rainfall in South Africa. Journal of Hydrometeorology **19** 127–142. http://doi.org/10.1175/JHM-D-17-0111.1.
- SOUSA MP, BLAMEY RC, REASON CJC, RAMOS AM and TRIGO R (2018) The "Day Zero" Cape Town drought and the poleward migration of moisture corridors. Environmental Research Letters **13.** https://doi.org/10.1088/1748-9326/aaebc7.
- RAMOS A, BLAMEY R, ALGARRA I, NIETO R, GIMENO L, TOME R, REASON CJC and TRIGO R (2019) From Amazonia to southern Africa: Atmospheric moisture transport through low level jets and atmospheric rivers. Annals of the New York Academy of Sciences **1436** 217–230. http://doi.org/10.1111/nyas.13960.

Two black South African students (R Rapolaki and D Morake) have conducted PhD research on aspects relating to the project, although they have not been directly funded by it.

CHAPTER 4: CONCLUDING REMARKS

An analysis of heavy rainfall events over the Limpopo River Basin during the summer has shown that these are more common from January to March than from October to December. A sharp rainfall gradient exists across the region, which is related to topography and distance from moisture sources, most obviously the Indian Ocean. Tropical extratropical cloud bands make the largest contribution overall and are most common in February. The second-largest contribution comes from tropical lows, which peak in February. Mesoscale convective systems can make a substantial contribution in any summer month, whereas cut-off lows are more likely in October and March. Ongoing work is considering the interannual variability of these synoptic systems and their contribution to heavy rainfall events here.

In terms of the interannual and interdecadal variability of the rainfall in the basin, an important aspect is the Botswana High. This high-pressure system is a mid-level anticyclone that forms in the austral spring over western tropical southern Africa and then moves south and strengthens during the summer so that its core region is located over central Namibia and western Botswana from December through to March. The relationships between low-frequency variability in this circulation system, regional rainfall, air temperature and sea surface temperature were examined. It is important to better understand this low-frequency variability, since it is likely to sometimes oppose and, at other times, reinforce trends in regional rainfall and temperature associated with global warming. As a result, until this anthropogenic forcing strongly dominates the natural variability signals, climate change signals over the region could be obscured to some extent in the near-term, posing challenges for the appropriate attribution and detection of climate change.

REFERENCES

ALLAN RJ, REASON CJC, LINDESAY JA and ANSELL TJ (2003) Protracted ENSO episodes over the Indian Ocean region. Deep-Sea Research Part II: Special Issue on Physical Oceanography of the Indian Ocean: From WOCE to CLIVAR **50** 2331–2347.

ANSELL TJ, REASON CJC, SMITH IN and KEAY K (2000) Evidence for decadal variability in southern Australian rainfall and relationships with regional pressure and sea surface temperature. International Journal of Climatology **20** 1113–1129.

BARIMALALA R, DESBIOLLES F, BLAMEY RC and REASON C (2018) Madagascar influence on the South Indian Ocean Convergence Zone, the Mozambique channel trough and southern African rainfall. Geophysical Research Letters **45** 380–389. https://doi.org/10.1029/2018GL079964

BEHERA SK and YAMAGATA T (2001) Subtropical SST dipole events in the southern Indian Ocean. Geophysical Research Letters **28** 327–330.

BLAMEY RC and REASON CJC (2012) Mesoscale convective complexes over southern Africa. Journal of Climate **25** 753–766**.**

BLAMEY RC and REASON CJC (2013) The role of mesoscale convective complexes in southern Africa summer rainfall. Journal of Climate **26** 1654–1668. http://dx.doi.org/10.1175/JCLI-D-12-00239.1.

BLAMEY RC, MIDDLETON C, LENNARD C and REASON CJC (2017) A climatology of potential severe convective environments across South Africa. Climate Dynamics **49** 2161–2178,

BLAMEY RC, KOLUSU SR, MAHLALELA P, TODD MC and REASON CJC (2018) The role of regional circulation features in regulating El Nino climate impacts over southern Africa: A comparison of the 2015/2016 drought with previous events. International Journal of Climatology **38** 4276–4295**. http://**doi.org/10.1002/joc.5668.

BOLVIN DT, ADLER RF, HUFFMAN GJ, NELKIN EJ and POUTIAINEN JP (2009) Comparison of GPCP monthly and daily precipitation estimates with high latitude gauge observations. Journal of Applied Meteorology and Climatology **48** 1843–1857.

COLBERG F, REASON CJC and RODGERS K (2004) South Atlantic response to ENSO induced climate variability in an OGCM. Journal of Geophysical Research **109.** http://doi.org/10.1029/2004JC002301.

COMPO GP, WHITAKER JS, SARDESHMUKH PD, MATSUI N, ALLAN RJ, YIN X, GLEASON BE, VOSE RS, RUTLEDGE G, BESSEMOULIN P, BRÖNNIMANN S, BRUNET M, CROUTHAMEL RI, GRANT AN, GROISMAN PY, JONES PD, KRUK MC, KRUGER AC, MARSHALL GJ, MAUGERI M, MOK HY, NORDLI Ø, ROSS TF, TRIGO RM, WANG XL, WOODRUFF SD and WORLEY SJ (2011) The twentieth century reanalysis project. Quarterly Journal of the Royal Meteorological Society **137** 1–28. http://doi.org/10.1002/qj.776.

COOK C, REASON CJC and HEWITSON BC (2004) Wet and dry spells within particular wet and dry summers in the South African summer rainfall region. Climate Research **26** 17–31.

CRÉTAT J, RICHARD Y, POHL B, ROUAULT M, REASON CJC and FAUCHEREAU N (2012) Recurrent daily rainfall patterns over South Africa and associated dynamics during the core of the austral summer. International Journal of Climatology **32** 261–273. http://doi.org/10.1002/joc.2266.

D'ABRETON PC and LINDESAY J (1993) Water vapour transport over southern Africa during wet and dry early and late summer months. International Journal of Climatology **13,** 151–170.

D'ABRETON PC and TYSON PD (1995) Divergent and non-divergent water vapour transport over southern Africa during wet and dry conditions. Meteorology and Atmospheric Physics **55** 47–59.

DEDEKIND Z, ENGELBRECHT FA and VAN DER MERWE J (2016) Model simulations of rainfall over southern Africa and its eastern escarpment. Water SA **42** 129–143.

DRIVER P and REASON CJC (2017) Variability in the Botswana High and its relationships with rainfall and temperature characteristics over southern Africa. International Journal of Climatology **37**. http://doi.org/10.1002/joc.5022.

DRIVER P, ABIODUN B and REASON CJC (2018) Modelling the precipitation response over southern Africa to the 2009/2010 El Niño using a stretched grid global atmospheric model. Climate Dynamics **52.** https://doi.org/10.1007/s00382-018-4362-5.

DYSON LL (2009) Heavy daily-rainfall characteristics over the Gauteng province. Water SA **35** 627–638.

DYSON LL and VAN HEERDEN J (2001) The heavy rainfall and floods over the northeastern interior of South Africa during February 2000. South African Journal of Science **97** 80–86.

DYSON LL, VAN HEERDEN J and SUMNER PD (2015) A baseline climatology of sounding-derived parameters associated with heavy rainfall over Gauteng, South Africa. International Journal of Climatology **35** 114–127.

ENGELBRECHT CJ, LANDMAN WA, ENGELBRECHT FA and MALHERBE J (2015) A synoptic decomposition of rainfall over the Cape south coast of South Africa. Climate Dynamics **44** 2589–2607.

FAVRE A, HEWITSON B, LENNARD C, CEREZO-MOTA R and TADROSS M (2013) Cut-off Lows in the South Africa region and their contribution to precipitation. Climate Dynamics **41** 2331–2351.

FAVRE A, HEWITSON B, TADROSS M, LENNARD C and CEREZO-MOTA R (2012) Relationships between cut-off lows and the semiannual and southern oscillations. Climate Dynamics **38** 1473–1487.

FITCHETT JM and GRAB SW (2014) A 66-year tropical cyclone record for south-east Africa: Temporal trends in a global context. International Journal of Climatology **34** 3604–3615.

FUNK C, PETERSON P, LANDSFELD M, PEDREROS D, VERDIN J, SHUKLA S, HUSAK G, ROWLAND J, HARISSON L, HOELL A and MICHAELSON J (2015) The climate hazards infrared precipitation with stations a new environmental record for monitoring extremes. Scientific Data **2** 150066.

GILLETT NP, KELL TD and JONES PD (2006) Regional climate impacts of the southern annular mode. Geophysical Research Letters **33.**

GRIMM AM and REASON CJC (2015) Intraseasonal teleconnections between South America and South Africa. Journal of Climate **28** 9489–9497.

HACHIGONTA S and REASON CJC (2006) Interannual variability in dry and wet spell characteristics over Zambia. Climate Research **32** 49–62.

HANSINGO K and REASON CJC (2009) Modelling the atmospheric response over southern Africa to SST forcing in the southeast tropical Atlantic and southwest subtropical Indian Oceans. International Journal of Climatology **29** 1001–1012.

HARRIS I and JONES PD (2015) CRU TS3.23: Climatic Research Unit (CRU) Time-Series (TS) Version 3.23 of high resolution gridded data of month-by-month variation in climate (Jan. 1901–Dec. 2014). Centre for Environmental Data Analysis, 9 November 2015. http://doi.org/10.5285/4c7fdfa6-f176-4c58-acee-683d5e9d2ed5.

HARRISON MSJ (1984) A generalized classification of South African summer rain-bearing synoptic systems. Journal of Climatology **4** 547–560.

HART NCG (2012) *Synoptic-scale rainfall patterns over southern Africa: Scale-interactions with large-scale modes of variability*. PhD thesis, University of Cape Town, Cape Town, South Africa.

HART NCG, REASON CJC and FAUCHEREAU N (2010) Tropical-extratropical interactions over southern Africa: Three cases of heavy summer season Rainfall. Monthly Weather Review **138** 2608—2623.

HART NCG, REASON CJC and FAUCHEREAU N (2013) Cloud bands over southern Africa: Seasonality, contribution to rainfall variability and modulation by the MJO. Climate Dynamics **41** 1199–1212. http://doi.org/10.1007/s00382-012-1589-4.

HART NCG, WASHINGTON R and REASON CJC (2018) On the likelihood of tropical–extratropical cloud bands in the south Indian convergence zone during ENSO events. Journal of Climate **31** 2797–2817.

HART RE and GRUMM RH (2001) Using normalized climatological anomalies to rank synoptic-scale events objectively. Monthly Weather Review **129** 2426–2442.

HERMES JC and REASON CJC (2005) Ocean model diagnosis of interannual co-evolving SST variability in the south Indian and Atlantic oceans. Journal of Climate **18** 2864–2882.

HIRST AC and HASTENRATH S (1983) Atmosphere-ocean mechanisms of climate anomalies in the Angola-tropical Atlantic sector. Journal of Physical Oceanography **13** 1146–1157.

HOELL A, FUNK C, ZINKE J and HARRISON L (2017) Modulation of the southern Africa precipitation response to the El Niño southern oscillation by the subtropical Indian Ocean dipole. Climate Dynamics **48** 2529–2540.

HUFFMAN GJ, ADLER RF, BOLVIN DT and GUOJUN G (2009) Improving the global precipitation record: GPCP Version 2.1. Geophysical Research Letters **36.**

IPCC (2013) *Climate change 2013: The physical science basis. Contribution of Working Group I to the Fifth Assessment Report of the Intergovernmental Panel on Climate Change,* Stocker TF, Qin D, Plattner G-K, Tignor M, Allen SK, Boschung J, Nauels A, Xia Y, Bex V and Midgley P, Cambridge University Press, Cambridge, UK and New York, NY, USA.

KALNAY E, KANAMITSU M, KISTLER R, COLLINS W, DEAVEN D, GANDIN L, IREDELL M, SAHA S, WHITE G, WOOLLEN J, ZHU Y, CHELLIAH M, EBISUZAKI W, HIGGINS W, JANOWIAK J, MO KC, ROPELEWSKI C, WANG J, LEETMAA A, REYNOLDS R, JENNE R and JOSEPH D (1996) The NCEP/NCAR 40-year reanalysis project. Bulletin of the American Meteorological Society **77** 437–471.

KNAPP KR, ANSARI S, BAIN CL, BOURASSA MA, DICKINSON MJ, FUNK C, HELMS CN, HENNON CC, HOLMES CD, HUFFMAN GJ, KOSSIN JP, LEE H-T, LOEW A and MAGNUSDOTTIR G (2011) Globally gridded satellite observations for climate studies. Bulletin of the American Meteorological Society **92** 893–907.

KNAPP KR, KRUK MC, LEVINSON DH, DIAMOND HJ and NEUMANN CJ (2010) The International Best Track Archive for Climate Stewardship (IBTrACS). Bulletin of the American Meteorological Society **91** 363–376.

LINDESAY JA (1988) South African rainfall, the southern oscillation and a southern hemisphere semi-annual cycle. Journal of Climatology **8** 17–30.

LYON B and MASON SJ (2007) The 1997–98 summer rainfall season in southern Africa. Part I: Observations. Journal of Climate **20** 5134–5148.

MAIDMENT RI, GRIMES D, ALLAN RP, TARNAVSKY E, STRINGER M, HEWISON T, ROEBELING R and BLACK ECL (2014) The 30 year TAMSAT African Rainfall Climatology and Time series (TARCAT) data set. Journal of Geophysical Research: Atmospheres **119** 10 619–10 644.

MALHERBE J, ENGELBRECHT FA, LANDMAN WA and ENGELBRECHT CJ (2012) Tropical systems from the southwest Indian Ocean making landfall over the Limpopo River basin, southern Africa: A historical perspective. International Journal of Climatology **32** 1018–1032.

MALHERBE JA, LANDMAN WA and ENGELBRECHT FA (2014) The bi-decadal rainfall cycle, southern annular mode and tropical cyclones over the Limpopo River basin, southern Africa. Climate Dynamics **42** 3121–3138.

MALHERBE J, DIEPPOIS B, MALULEKE P, VAN STADEN M and PILLAY DL (2016) South African droughts and decadal variability. Natural Hazards. http://doi.org/10.1007/s11069-015-1989-y.

MANHIQUE A, REASON CJC, RYDBERG L and FAUCHEREAU N (2011) ENSO and Indian Ocean sea surface temperatures and their relationships with tropical temperate troughs over Mozambique and the southwest Indian Ocean. International Journal of Climatology **31** 1-13. http://doi.org/10.1002/joc.2050**.**

MANHIQUE A, REASON C.J.C., B. SILINTO, J. ZUCULA, I. RAIVA, F. CONGOLO, A. F. MAVUME, 2015: Extreme rainfall and floods in southern Africa in January 2013 and associated circulation patterns. Natural Hazards **77** 679–691**.** http://doi.org/10.1007/s11069-015-1616-y.

MARSHALL GJ (2003) Trends in the southern annular mode from observations and reanalyses. Journal of Climate **16** 4134–4143.

MASON SJ (1990) Temporal variability of sea surface temperature around southern Africa: A possible forcing mechanism for the eighteen-year rainfall oscillation? South African Journal of Science **86** 243–252.

MASON SJ (1995) Sea-surface temperature – South African rainfall associations, 1910–1989. International Journal of Climatology **15** 119–135.

MASON SJ and JURY MR (1997) Climatic variability and change over southern Africa: A reflection on underlying processes. PPG: Earth and Environment **21** 23–50.

MOSASE E and AHIABLAME L (2018) Rainfall and temperature in the Limpopo River basin, southern Africa: Means, variations and trends from 1979 to 2013. Water **10.**

MATARIRA CH (1990) Drought over Zimbabwe in a regional and global context. International Journal of Climatology **10** 609–625.

MULENGA HM, ROUAULT M and REASON CJC (2003) Dry summers over NE South Africa and associated circulation anomalies. Climate Research **25** 29–41.

MUNDAY C and WASHINGTON R (2017) Circulation controls on southern African precipitation in coupled models: The role of the Angola Low. Journal of Geophysical Research **122**. http://doi.org/10.1002/2016JD025736.

MUÑOZ ÁG, GODDARD L, ROBERTSON AW, KUSHNIR Y and BAETHGEN W (2015) Cross-time scale interactions and rainfall extreme events in southeastern South America for the austral summer. Part I: Potential predictors. Journal of Climate **28** 7894–7913.

NICHOLSON SE and KIM J (1997) The relationship of the El Niño – southern oscillation to African rainfall. International Journal of Climatology **17** 117–135.

POHL B, FAUCHEREAU N, RICHARD Y, ROUAULT M and REASON CJC (2009) Interactions between synoptic, intraseasonal and interannual convective variability over southern Africa. Climate Dynamics **33** 1033–1050. http://doi.org/10.1007/s00382-008-0485-4.

POHL B, FAUCHEREAU N, REASON CJC and ROUAULT M (2010) Relationships between the Antarctic oscillation, the Madden-Julian oscillation and ENSO, and consequences for rainfall analysis. Journal of Climate **23** 238–254. http://doi.org/10.1175/2009JCLI2443.1.

RAMOS AM, TRIGO RM and LIBERATO ML (2017) Ranking of multi-day extreme precipitation events over the Iberian Peninsula. International Journal Climatology **37** 607–620.

RAMOS AM, TRIGO RM and LIBERATO ML (2014) A ranking of high-resolution daily precipitation extreme events for the Iberian Peninsula. Atmospheric Science Letters **15** 328–334.

RAPOLAKI RS and REASON CJC (2018) Tropical storm Chedza and associated floods over south-eastern Africa. Natural Hazards **93** 189–217.

RAPOLAKI R, BLAMEY RC, HERMES J and REASON CJC (2019) A classification of synoptic weather patterns linked to extreme rainfall over the Limpopo River basin in southern Africa. Climate Dynamics **53** 2265–2279. http://doi.org/10.1007/s00382-019-04829-7.

RATNA SB, BEHERA S, RATNAM JV, TAKAHASHI K and YAMAGATA T (2012) An index for tropical temperate troughs over southern Africa. Climate Dynamics **41** 421–441.

REASON CJC (1998) Warm and cold events in the southeast Atlantic/southwest Indian Ocean region and potential impacts on circulation and rainfall over southern Africa. Meteorology and Atmospheric Physics **69** 49–65.

REASON CJC (1999) Interannual warm and cool events in the subtropical/mid-latitude south Indian Ocean region. Geophysical Research Letters **26** 215–218.

REASON CJC (2001) Subtropical Indian Ocean SST dipole events and southern African rainfall. Geophysical Research Letters **28** 225–228.

REASON CJC (2002) Sensitivity of the southern African circulation to dipole SST patterns in the South Indian Ocean. International Journal of Climatology **22** 377–393.

REASON CJC and MULENGA HM (1999) Relationships between South African rainfall and SST anomalies in the south west Indian Ocean. International Journal of Climatology **19** 1651–1673.

REASON CJC, ALLAN RJ, LINDESAY JA and ANSELL TJ (2000) ENSO and climatic signals across the Indian Ocean basin in the global context: Part I, interannual composite patterns. International Journal of Climatology **20** 1285–1327.

REASON CJC and ROUAULT M (2002) ENSO-like decadal patterns and South African rainfall. Geophysical Research Letters **29 (13)**. http://doi.org/10.1029/2002GL014663.

REASON CJC and KEIBEL A (2004) Tropical cyclone Eline and its unusual penetration and impacts over southern Africa. Weather and Forecasting **19 (5)** 789–805.

REASON CJC and JAGADHEESHA D (2005) A model investigation of recent ENSO impacts over southern Africa. Meteorology and Atmospheric Physics: Special Issue on Regional Climate **89** 181–205. http://doi.org/10.1007/s00703-005-0128-9.

REASON CJC, LANDMAN W, TENNANT W (2006) Seasonal to decadal prediction of southern African climate and its links with variability of the Atlantic Ocean. Bulletin of the American Meteorological Society **87** 941–955.

REASON CJC (2007) Tropical cyclone Dera, the unusual 2000/01 tropical cyclone season in the southwest Indian Ocean and associated anomalies in southern Africa. Meteorology and Atmospheric Physics: Special Issue on Tropical Cyclones **97** 273–290. http://doi.org/10.1007/s00703-007-0259-2.

REASON CJC (2016) The Bolivian, Botswana and Bilybara Highs and southern hemisphere drought/floods. Geophysical Research Letters **43** 1280–1286. http://doi.org/10.1002/2015GL067228.

REASON CJC (2019) Low frequency variability in the Botswana High and southern African regional climate. Theoretical and Applied Climatology **137** 1321–1334. http://doi.org/10.1007/s00704-018-2661-8.

RICHARD Y, FAUCHEREAU N, POCCARD I, ROUAULT M and TRZASKA S (2001) 20th century droughts in southern Africa: Spatial and temporal variability, teleconnections with oceanic and atmospheric conditions. International Journal of Climatology **21** 873–885.

ROUAULT M, WHITE SA, REASON CJC and LUTJEHARMS JRE (2002) Ocean-atmosphere interaction in the Agulhas current and a South African extreme weather event. Weather and Forecasting **17** 655–669.

ROUAULT M, FLORENCHIE P, FAUCHEREAU N and REASON CJC (2003) South east Atlantic warm events and southern African rainfall. Geophysical Research Letters **30 (5).** http://doi.org/10.1029/2002GL014840.

SCHNEIDER U, FUCHS T, MEYER-CHRISTOFFER A and RUDOLF B (2008) Global precipitation analysis products of the GPCC.Global Precipitation Climatology Centre (GPCC), Deutscher Wetterdienst. ftp://ftp-anon.dwd.de/pub/data/gpcc/PDF/GPCC_intro_products_2008.pdf.

SINGLETON AT and REASON CJC (2006) Numerical simulations of a severe rainfall event over the Eastern Cape coast of South Africa: Sensitivity to sea surface temperature and topography. Tellus A: Dynamic Meteorology and Oceanography **58** 335–367.

SINGLETON AT and REASON CJC (2007a) A numerical model study of an intense cut-off low pressure system over South Africa. Monthly Weather Review **135** 1128–1150.

SINGLETON AT and REASON CJC (2007b) Variability in the characteristics of cut-off low pressure systems over subtropical southern Africa. International Journal of Climatology **27** 295–310.

SMITH TM and REYNOLDS RW (2004) Improved extended reconstruction of SST (1854–1997). Journal of Climate **17** 2466–2477.

TADROSS MA, HEWITSON BC and USMAN MT (2005) The interannual variability of the onset of the maize growing season over South Africa and Zimbabwe. Journal of Climate **18** 3356–3372.

TALJAARD JJ (1985) *Cut-off lows in the South African region*. South African Weather Bureau Technical Note 14, 153, South African Weather Bureau, Pretoria, South Africa.

TODD MC and WASHINGTON R (1998) Extreme daily rainfall in southern African and southwest Indian Ocean tropical-temperate links. South African Journal of Science **94** 64–70.

TODD MC, WASHINGTON R and PALMER PI (2004) Water vapour transport associated with tropical-temperate trough systems over southern Africa and the southwest Indian Ocean. International Journal of Climatology **24** 555–568.

TYSON PD, DYER TGJ and MAMETSE MN (1975) Secular changes in South African rainfall: 1880 to 1972. Quarterly Journal of the Royal Meteorological Society **101** 817–833.

TYSON PD, COOPER GRJ and MCCARTHY TS (2002) Millenial to multidecadal variability in the climate of southern Africa. International Journal of Climatology **22** 1105–1117.

UNGANAI L and MASON S (2002) Long-range predictability of Zimbabwe summer rainfall. International Journal of Climatology **22** 1091–1103.

USMAN MT and REASON CJC (2004) Dry spell frequencies and their variability over southern Africa. *Climate Research* **26** 199–211.

VITART F, ANDERSON D and STOCKDALE T (2003) Seasonal forecasting of tropical cyclone landfall over Mozambique. Journal of Climate **16** 3932–3945.

WALKER ND (1990) Links between South African summer rainfall and temperature variability of the Agulhas and Benguela current systems. Journal of Geophysical Research **95** 3297–3319.

WASHINGTON R and TODD M (1999) Tropical-temperate links in southern Africa and southwest Indian Ocean satellite-derived daily rainfall. International Journal of Climatology **19** 1601–1616.

WASHINGTON R and PRESTON A (2006) Extreme wet years over southern Africa: Role of Indian Ocean sea surface temperatures. Journal of Geophysical Research **111**. http://doi.org/10.1029/2005JD006724.

WELDON D and REASON CJC (2014) Variability of rainfall characteristics over the south coast region of South Africa. Theoretical and Applied Climatology **115** 177–185. http://doi.org/10.1007/s00704-013-0882-4.